Energies **2014**, *7*, 4033-4053; doi:10.3390/en7064033

OPEN ACCESS

energies

ISSN 1996-1073

www.mdpi.com/journal/energies

Article

An Intelligent Fuzzy Logic Controller for Maximum Power Capture of Point Absorbers

Mohammed Jama [1], Addy Wahyudie [1,*], Ali Assi [2] and Hassan Noura [1]

[1] Electrical Engineering Department, United Arab Emirates University, Al Ain, P.O. Box 15551, UAE; E-Mails: m.jama@uaeu.ac.ae (M.J.); hnoura@uaeu.ac.ae (H.N.)

[2] Department of Electrical and Electronics Engineering, Lebanese International University, Beirut, P.O. Box 146404, Lebanon; E-Mail: ali.assi@liu.edu.lb

* Author to whom correspondence should be addressed; E-Mail: addy.w@uaeu.ac.ae; Tel.: +971-3-713-6582; Fax: +971-3-713-4970.

Received: 13 March 2014; in revised form: 29 May 2014 / Accepted: 13 June 2014 / Published: 24 June 2014

Abstract: This article presents an intelligent fuzzy logic controller (FLC) for controlling single-body heaving wave energy converter (WEC) or what is widely known as "Point Absorber". The controller aims at maximizing the energy captured from the sea waves. The power take-off (PTO) limitations are addressed implicitly in the fuzzy inference system (FIS) framework. In order to enhance the WEC power capturing bandwidth and make it less susceptible to wave environment irregularities and the system parametric uncertainties, the controller is built to have a self-configurable capability. This also eliminates the need to repeatedly run *in-situ* tuning procedure of the fuzzy controller or switch between several controllers based on the operating conditions. The fuzzy membership functions (MFs) are optimally tuned using particle swarm optimization (PSO) algorithm. To alleviate the computational burden associated with performing on-line optimization, the fuzzy controller is tuned at a rate significantly lower than the system sampling time. The suggested PSO-FLC has shown promising results compared with the fixed structure fuzzy logic controller (FS-FLC) and other passive control strategies. Several computer simulations were carried out to evaluate the controller effectiveness by applying different sea-states and analyzing the resultant WEC dynamics.

Keywords: wave energy; fuzzy logic; power take-off; particle swarm optimization

---

1. Introduction

Wave energy is deemed to be one of the most promising renewable energy resources, with an estimated global potential of 2 TW [1]. The first attempts to harness wave energy dates back to 1940s, however, serious governmental projects on wave energy have started after the oil crisis in 1973 [2]. Apart from being abundant, wave energy is a concentrated form of solar energy, with power density of approximately 2 kW/m^2 [1]. Wave energy converters (WEC) are used to convert the mechanical power of the traveling sea waves to electrical power that can be fed to the grid. WECs vary according to many aspects, that is, the installation site (*i.e.*, nearshore or offshore), the principle of operation (*i.e.*, oscillating, pitching, *etc*.) and the deployed power take-off (PTO) mechanism. The economic feasibility of the WEC depends on the wave potential at the installation site, the efficiency of the PTO, and the effectiveness of the used control strategy, along with other factors such as installation and maintenance costs [2,3].

Recently, an extensive research effort has been dedicated to the area of WEC control to maximize the exploited wave energy, while ensuring that the device is operating safely and within its physical and thermal limits. Falnes and Budal pioneered the efforts which led to the important principle of WEC maximum power absorption [2,3]. A major drawback of optimal control strategies are their non-causal nature [4]. Control techniques such as amplitude and phase control are proposed as a more practical alternative to optimal control strategies [4]. In [5], a passive control strategy that considers the linear generator copper losses is implemented. An adaptive controller based on constrained average power maximization method is proposed in [6]. The suggested technique highlighted the importance of properly selecting and tuning the control strategy and how that affects the ratings of the deployed PTO components (e.g., generator, power electronics, *etc.*). Feedback linearization is a control strategy which provides a linear system dynamics instead of non-linear dynamics of the WEC. However, in practice, non-linear dynamics (forces) will never be so accurately cancelled, which deteriorate the performance of these control strategies [7]. Latching control is another technique based on phase control, where the buoy is latched and unlatched at predetermined intervals, hence, the absorbed power is maximized and the power reversals are minimized. Computing the latching intervals is rather a challenging task, knowing the irregularity of the sea waves [7]. Numerous studies proposed the use of neural networks to accurately model the non-linear dynamics of WECs. Elman dynamic neural network is employed to model the dynamics of WEC, where the wave excitation force and the PTO force are selected as inputs and the buoy velocity as output [8]. In [9], model predictive controller (MPC) strategy is implemented to control the motion of a heaving WEC; however numerous assumptions and simplifications have been made by the author, such as adopting simplified hydrodynamic models. In [10], the authors proposed robust fuzzy controller, which combines between a fuzzy controller responsible of short-term wave fluctuations and GA optimization which handles the long-term wave fluctuations, along with an offline robust controller, which minimizes the effects of uncertainties in the control strategy.

In this paper, an intelligent fuzzy logic based controller is proposed to control a point absorber WEC. This work is an extension of the preliminary results presented in [11,12]. FLCs usually offer better performance for systems which suffer from model complexity, stochastic behavior, parametric variations and/or disturbances compared to classical model based controllers such as PID controller [13]. The

FLC rule-base is constructed based on physical laws, namely, maximum power transfer theorem. The controller is of the reference-less type, that is, no optimum velocity trajectory is needed. Furthermore, in order to address the tuning problem and add a certain level of robustness to the FLC, it is equipped with particle swarm optimization (PSO) algorithm, that optimally tune the fuzzy membership functions, which eliminates the need for building another optimal robust controller. This self-configurable nature of the controller will not only give it a degree of robustness towards parametric uncertainties, but also widen the operating region of the FLC, without the need to re-construct the fuzzy inference system. PSO is deployed due to its simplicity, flexibility, and fast convergence time. The controller ability to maximize the absorbed energy is assessed. Also the controller behavior to parameter variations is assessed at different wave environments. The paper is organized as follows. Section 2 discusses the dynamics and modeling of point absorber. Section 3 describes the controller design. Section 4 includes the simulation results and the corresponding discussions. Section 5 is devoted to conclusions.

2. Heaving WEC Dynamics

In this work, the Uppsala University point absorber design is considered as shown in Figure 1. The device is a seabed-reacting axisymmetric heaving system, which consists of a floating spherical body (buoy) connected to a permanent magnet linear generator (PMLG) through a rod. Conventionally, the PMLG, which is installed on the seabed, is composed of a translator that moves in one degree of freedom, on which an alternating polarity permanent magnet is mounted. The linear motion of the translator surrounded with a fixed stator windings, will induce voltage on the armature windings [14]. Apart from electricity generation, the PMLG is utilized to damp the oscillation of the buoy in a controlled manner; hence the energy absorption of the WEC depends on the damping capabilities of the PMLG [4,15]. Besides, controlled excursions are applied on the buoy by the PMLG to limit the damage that could occur due to extreme waves.

Figure 1. Heaving point absorber structure.

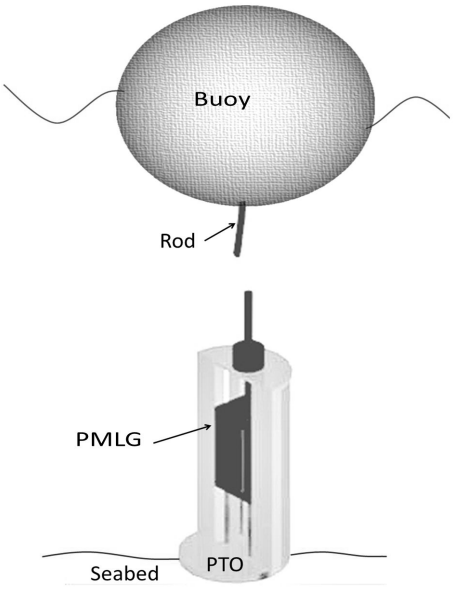

The movement of the WEC oscillating body is governed by the forces resulting from the wave-body interactions and the forces applied by the PTO and mooring mechanisms. There is an array of forces that is experienced by the oscillating body and an equal number of reaction forces as stated in Newton's third law [16]. Nevertheless, forces acting on the floating body are the ones of interest when modeling the motion of WECs. Based on linear wave theory, where only small wave amplitudes are considered, the forces acting on the oscillating body are [3,10]:

- The wave excitation force, $f_e(t)$, is simply the force exerted by the incident waves on the WEC floater assuming that it is held motionless;
- The hydrodynamic radiation force, $f_r(t)$, is the force that both the oscillating body and the surrounding fluid apply on each, due to the alteration of the pressure field over the submerged portion of the buoy as the waves are created;
- The buoyancy stiffness force, $f_b(t)$, which results from the imbalance between the floater weight and the weight of the displaced fluid during oscillation. The buoyancy force is a function of the buoy displacement $z(t)$, water density ρ, the gravitational acceleration g, and the water plane area A_w, such that $f_b(t) = \rho g A_w z(t)$. Note that the water plane area A_w is assumed to be fixed for the sake of simplicity. Therefore, the buoyancy stiffness coefficient is defined as $S_b = \rho g A_w$;
- The drag force, $f_d(t)$, which is a nonlinear resistive force exerted by the water on the reciprocating buoy, where $f_d(t) = 0.5\rho A_w C_D|\dot{z}(t)|\dot{z}(t)$, where C_D is the drag coefficient;
- The mooring system force, $f_m(t)$, is a force applied on the buoy by a tight mooring lines. In this study, in order to keep the buoy in place, it is moored to two neighboring floating mooring points (e.g., small buoys). The mooring force is modeled to have a nonlinear spring effect, $f_m(t) = 2S_m z(t)(1 - L_m/\sqrt{L_m^2 + z(t)^2})$, where S_m and L_m are the mooring cable stiffness and the cable horizontal length, respectively [17,18];
- The restoring force, $f_{rs}(t)$, which represents the force applied by the auxiliary spring units installed between the translator of the PMLG and the system's point of interaction at the seabed. $f_{rs}(t)$ is modelled as a spring force, such as, $f_{rs}(t) = S_{rs} z(t)$, where S_{rs} represents the spring stiffness coefficient;
- The losses force, $f_l(t)$, which includes the losses due to friction, viscosity, and non-ideal PTO mechanisms. In practice, this force is nonlinear and time variant, however, for convenience, it is modeled as a linear time-invariant resistive force, that is $f_l(t) = R_l \dot{z}(t)$, where R_l represents the losses damping coefficient;
- The input force, $f_u(t)$, which is the force applied by the PTO system on the WEC. This force is usually governed by a controller to maximize the captured energy.

Since this research is only discussing point absorbers WECs and for the sake of simplicity, only one degree of freedom of motion (heave) will be considered. The system equation of motion can be described as

$$f_e(t) - f_r(t) - f_b(t) - f_{rs}(t) - f_d(t) - f_m(t) - f_l(t) + f_u(t) = m\ddot{z}(t) \quad (1)$$

where m is the total mass of the WEC floater and the linear generator translator, $\ddot{z}(t)$ is the gravitational acceleration of the floater. As proposed by Cummins, the linear time domain representation of the zero forward speed radiation force could be written as [19]

$$f_r(t) = m_\infty \ddot{z}(t) + \int_0^t k_r(t-\tau)\dot{z}(\tau)\,\mathrm{d}\tau \tag{2}$$

The first term models the fluid pressure forces due to the floater acceleration, where $m_\infty = \lim_{\omega\to\infty} M_r(\omega)$, which is the radiation added mass at infinite frequency. The convolution term represents the fluid memory effects which dissipates part of the incident power away from the floating body as a result of the destructive interference between the future incoming waves and the current radiated waves. The convolution kernel, $k_r(t)$ is called the retardation function or the radiation impulse function. The frequency domain radiation damping $R_r(\omega)$ and added mass $M_r(\omega)$ can be related to the radiation impulse function as follows [20]:

$$R_r(\omega) = \int_0^\infty k_r(t)\cos(\omega t)\,\mathrm{d}t \tag{3}$$

$$M_r(\omega) = m_\infty - \frac{1}{\omega}\int_0^\infty k_r(t)\sin(\omega t)\,\mathrm{d}t \tag{4}$$

The values of $R_r(\omega)$ and $M_r(\omega)$ for various angular frequencies have been evaluated by numerically solving the buoy's frequency domain radiation problem using WAMIT$^{\mathrm{TM}}$ [21].

2.1. State Space Representation of the WEC Model

Several works have been conducted on how to handle the radiation convolution term [22,23]. In this paper, the method adopted in [22] has been used, where the radiation convolution term is approximated by fourth order linear state space model as follows

$$\dot{\mathbf{q}}(t) = \mathbf{A}_k\mathbf{q}(t) + \mathbf{B}_k\dot{z}(t) \tag{5}$$

$$\int_0^t k_r(t-\tau)\dot{z}(\tau)\mathrm{d}\tau \approx \mathbf{C}_k\mathbf{q}(t) \tag{6}$$

where $\mathbf{q}(t) \in \mathbb{R}^{4\times 1}$ is the state vector; the buoy velocity $\dot{z}(t) \in \mathbb{R}^{1\times 1}$ is the input and the radiation force $f_r(t) \in \mathbb{R}^{1\times 1}$ is the model output. $\mathbf{A}_k$, $\mathbf{B}_k$ and $\mathbf{C}_k$ are the state matrix, input matrix and output matrix, respectively. Equation (6) can be easily lumped into Equation (1) to formulate the state space model of the WEC system, hence

$$\begin{aligned}\ddot{z}(t) =& \frac{1}{m+m_\infty}[f_e(t) - \mathbf{C}_k\mathbf{q}(t) - (S_b+S_{rs})z(t) - 0.5\rho A_w C_D|\dot{z}(t)|\dot{z}(t) - R_l\dot{z}(t) - 2S_m z(t)(1-\\ & L_m/\sqrt{L_m^2+z(t)^2}) + f_u]\end{aligned} \tag{7}$$

the state vector $\mathbf{x}(t) \in \mathbb{R}^{6\times 1}$ can be chosen to be $\mathbf{x}(t) = [z(t)\ \dot{z}(t)\ \mathbf{q}(t)^T]^T$, which is assumed to be entirely measurable with initial conditions of $\mathbf{x}(0) = [0\ 0\ \mathbf{0}_{1\times 4}]^T$. The inputs to the system consist of the wave excitation force $f_e(t)$, which is treated as a measurable un-manipulated input and the input force $f_u(t)$, which can be manipulated by the controller to achieve optimum performance. The wave excitation force $f_e(t)$ is approximated using a method similar to that used to approximate the radiation force $f_r(t)$. In this study, the model output $y(t)$ is the buoy vertical velocity $\dot{z}(t)$. The overall model can be written as

$$\begin{aligned}
\dot{x}_1 &= x_2 \\
\dot{x}_2 &= \frac{1}{m+m_\infty}[f_e(t) - \mathbf{C}_k\mathbf{x}_3 - (S_b+S_{rs})x_1 - 0.5\rho A_w C_D|x_2|x_2 - \\
&\quad R_l x_2 - 2S_m x_1(1 - L_m/\sqrt{L_m^2+x_1^2}) + f_u(t)] \\
\dot{\mathbf{x}}_3 &= \mathbf{A}_k\mathbf{x}_3 + \mathbf{B}_k x_2 \\
y &= x_2
\end{aligned} \tag{8}$$

Alternatively, the model can be re-formed into the compact state space representation as

$$\dot{\mathbf{x}} = \mathbf{A}\mathbf{x} + \mathbf{B}(w(t) + u(t)) + \mathbf{\Theta} \tag{9}$$

$$y = \mathbf{C}\mathbf{x} \tag{10}$$

where

$$\mathbf{A} = \begin{bmatrix} 0 & 1 & \mathbf{0}_{1\times 4} \\ \frac{-(S_b+S_{rs})}{m+m_\infty} & \frac{-R_l}{m+m_\infty} & \frac{-\mathbf{C_k}}{m+m_\infty} \\ \mathbf{0}_{4\times 1} & \mathbf{B_k} & \mathbf{A_k} \end{bmatrix} \in \mathbb{R}^{6\times 6}, \mathbf{B} = \begin{bmatrix} 0 \\ \frac{1}{m+m_\infty} \\ \mathbf{0}_{4\times 1} \end{bmatrix} \in \mathbb{R}^{6\times 1}$$

$$\mathbf{\Theta} = \begin{bmatrix} 0 \\ \frac{-0.5\rho A_w C_D|x_2|x_2 - R_l x_2 - 2S_m x_1(1-L_m/\sqrt{L_m^2+x_1^2})}{m+m_\infty} \\ \mathbf{0}_{4\times 1} \end{bmatrix} \in \mathbb{R}^{6\times 1}, \mathbf{C} = \begin{bmatrix} 0 & 1 & \mathbf{0}_{1\times 4} \end{bmatrix} \in \mathbb{R}^{1\times 6}$$

Note that $u(t)$, $w(t)$, and $\mathbf{\Theta}$ represent the input force, the wave excitation force, and the nonlinear vector, respectively.

3. Controller Design

To bring down the system's operating frequency to that of the most energetic wave frequencies ($\omega < 1$ rad/s), an appropriate external force must be first determined by a controller and then applied on the buoy. The controller alters $f_u(t)$ by continuously adjusting the change of damping R_u and spring stiffness S_u coefficients, such as [16]

$$f_u(t) = -R_u\dot{z}(t) - S_u z(t) \tag{11}$$

3.1. Fixed Structure Fuzzy Logic Controller (FS-FLC)

Two-input two-output fuzzy controller is implemented. Fuzzy controllers have received great appreciation in industry recently [24–26]. That is due to wide range of advantages that they offer, if they are implemented properly. FLCs are independent of the mathematical model of the plant under investigation; instead they are based on human expertise. Moreover, fuzzy based controllers offer a more flexible alternative for control designers, that is, the input and output variables can be given different treatments to counteract inherent nonlinearities or environment disturbances [24]. The main drawback of FLCs is that there is no systematic procedure to design and tune the fuzzy inference system (FIS) parameters [27].

Based on the principle of amplitude and phase control [16], the proposed fuzzy controller accepts two input variables, the first input is the amplitude difference between the measured wave elevation and the measured buoy displacement $\Delta A = \eta(t) - z(t)$, while the second input is the phase difference between the computed excitation force and the measured buoy heave velocity $\Delta\theta = \theta_{f_e}(t) - \theta_{\dot{z}}(t)$. The phase difference is computed by a windowed cross correlation method between the two signals; where the output of the cross correlation varies between -1 and 1. Due to the windowed computation of the phase shift input signal, it is altered less often compared to the amplitude difference input signal. Practically, measurements of the wave elevation can be taken by another buoy installed close to the WEC. The FLC outputs two crisp variables namely, the PMLG damping and spring stiffness coefficients. Seven fuzzy sets are assigned for each input and output variable as shown in Table 1. Gaussian MF is chosen for all input and output variables with different universe of discourse ranges. Each Gaussian MF is defined by the mean m and standard deviation σ. The FLC inference rule-base is divided into two groups, the first are those linking the inputs to the required damping coefficient and the second set of rules relates the inputs to the required spring stiffness.

Table 1. Fuzzy rulebase.

IF	ΔA is **Z**	THEN	R_u is **Z**
	ΔA is **PS**		R_u is **NS**
	ΔA is **PM**		R_u is **NM**
	ΔA is **PB**		R_u is **NB** and S_u is **PB**
	ΔA is **NS**		R_u is **PS**
	ΔA is **NM**		R_u is **PM** and S_u is **NM**
	ΔA is **NB**		R_u is **PB** and S_u is **NB**
IF	$\Delta\theta$ is **Z**	THEN	S_u is **Z**
	$\Delta\theta$ is **PS**		S_u is **PS**
	$\Delta\theta$ is **PM**		S_u is **PM**
	$\Delta\theta$ is **PB**		S_u is **PB**
	$\Delta\theta$ is **NS**		S_u is **NS**
	$\Delta\theta$ is **NM**		S_u is **NM**
	$\Delta\theta$ is **NB**		S_u is **NB**

Z: Zero; **PS**: Positive small; **NS**: Negative small; **PM**: Positive medium; **NM**: Negative medium; **PB**: Positive big; **NB**: Negative big.

Without the input PTO force, the spring effect dominates the oscillating system intrinsic impedance. Therefore, by controlling the PMLG stiffness force, the velocity can be made less leading (or nearly in

phase) compared to the excitation force, which results in higher excursions and more energy absorption. The opposite can be done to suppress the buoy excursions. Also if ΔA is positive, the damping supplied by the PMLG is reduced, while more damping is applied when ΔA is negative. The FLC uses the Mamdani type FIS with the center of gravity (centroid) method for defuzzification. To limit the controlled machinery force, the FLC universe of discourse of R_u is set to $[0, 1 \times 10^5]$, while the universe of discourse of S_u is set to $[0, 1.2 \times 10^6]$. Note that the universe of discourse ranges for the output signals are set based on the characteristics of the used actuator. The universe of discourse for ΔA and $\Delta\theta$ are $[-5, 5]$ and $[-1, 1]$, respectively.

Due to the absence of systematic methods to determine the input and output MFs parameters, they have been chosen by trial and error; however that does not guarantee a decent performance of the WEC at diverse sea conditions. Therefore a method to continuously update the MFs to achieve optimum WEC operation is required. From here after, the developed FLC will be referred to as fixed structure FLC (FS-FLC) in order to differentiate it from its self-configurable counterpart that is discussed next.

3.2. PSO-Fuzzy Logic Controller (PSO-FLC)

Much research work has been devoted to the subject of FLC online optimization [28–30]. A proper selection of the FLC rule base and/or the MFs parameters would significantly improve the control action while the system is operating.

PSO algorithms have been utilized in many engineering problems [31,32]. The fact that they are simple, fast and computationally efficient made them an attractive tool in many complex optimization problems, especially if the variable to be optimized has a high dimension. Many research works have indicated that in many applications PSO has better convergence speed compared to other population-based algorithms such as genetic algorithm (GA) [33]. The PSO principle has been inspired from the flocking bird behavior, where each bird resembles a solution (particle) in the search space. Naturally, the birds rely on their own experience and their social relations with other birds to find food [34]. Similarly, the particles in the algorithm fly around in a d-dimensional space to find an optimum solution for a given problem using their own and other particles experience. Each particle is assessed by evaluating a fitness function, such that the swarm will gradually lean towards an optimum solution at which the minimum or maximum value of the fitness function is attained. During the search, each particle's velocity and position is updated as shown in Equations (12) and (13) [35]

$$v_i^d(j+1) = \omega_n v_i^d(j) + \beta_1 r_1(\hat{p}_i^d - x_i^d(j)) + \beta_2 r_2(\hat{g}^d - x_i^d(j)) \tag{12}$$

$$x_i^d(j+1) = x_i^d(j) + v_i^d(j+1) \tag{13}$$

At the iteration number j, the variables $v_i^d(j+1)$ and $v_i^d(j)$ are the d^{th} dimensional i^{th} particle updated and current velocity, respectively. While $x_i^d(j+1)$ and $x_i^d(j)$ are the d^{th} dimensional i^{th} particle updated and current position, respectively.The parameters ω_n, β_1 and β_2 are the inertia weight, cognitive attraction and social attraction parameters, respectively. While $\hat{p}_i^d$ is the i^{th} particle previous best position and $\hat{g}^d$ is the global best position among all particles in the d-dimensional swarm. r_1 and r_2 are random weights in the range $[0, 1]$. The particle inertia weight ω_n determines the impact of the current particle velocity

on the updated (future) particle dynamics.β_1 and β_2 decide the size of the neighborhood at which the searching is taking place.

In this work, each particle contains the values of the inputs and outputs MFs parameters, namely the Gaussian MF mean and standard deviation. The PSO algorithm searches in a pre-determined bounded searching space for the optimum solution that maximizes the absorbed real power. After initiating the particles with values within the specified boundaries, the goodness of the new particles are evaluated by updating the fuzzy controller and checking the WEC system response through computing a cost function. The dynamics of each particle is updated at every iteration using Equations (12) and (13). This procedure continues until an optimum set of MFs parameters are obtained. Table 2 summarizes the PSO algorithm.

Table 2. Pseudo code of the PSO algorithm.

Initialize the population position vector $x_i^d = (x_1^d, x_2^d, \ldots, x_N^d)^T$ and velocity vector $v_i^d = (v_1^d, v_2^d, \ldots, v_N^d)^T$ randomly at $j = 1$, N is the population size
while(iteration limit is reached)
$j = j + 1$
for loop over all d^{th} dimensional N particles
Update v_i^d using Equation (12)
Update x_i^d using Equation (13)
Adjust the controller FIS
Evaluate the objective function (Equation (16)) for current x_i^d
Determine the current best for each particle $\hat{p}_i^d$
end for loop
Determine the current global best $\hat{g}^d$
end while
Output the final $\hat{g}^d$ and $\hat{p}_i^d$

The dimension of each particle in the swarm is 56, which is the total number of mean and standard deviation parameters that need to be tuned (*i.e.*, 14 particles for each input and output variable) . The PSO algorithm attempts to adaptively tune the parameters of the FLC MFs by adjusting the change of the mean Δm and the standard deviation $\Delta\sigma$ parameters from their nominal settings (*i.e.*, m_o and σ_o), used in FS-FLC as shown in Figure 2. Each particle $\chi \in \mathbb{R}^{1\times 56}$ is represented as follows

$$\chi = [\Gamma_1, \Gamma_2, \Gamma_3, \Gamma_4] \tag{14}$$

where Γ_1 and Γ_2 comprise the fuzzy MFs parameters of the first and second input variables, while Γ_3 and Γ_4 include the output variables MFs parameters, that is

$$\Gamma_1 = [\Delta m_1, \Delta m_2, \ldots, \Delta m_7, \Delta\sigma_1, \Delta\sigma_2, \ldots, \Delta\sigma_7] \in \mathbb{R}^{1\times 14} \tag{15}$$

Hard upper and lower bounds are set for particle's parameters to limit the search space, that is, $\Delta m \in [\Delta m_{low}\ \Delta m_{up}]$ and $\Delta\sigma \in [\Delta\sigma_{low}\ \Delta\sigma_{up}]$. These bounds are picked arbitrarily as a percentage of the nominal values of the MF parameters. Each input/output fuzzy variable could have its own MF

parameters bounds. The objective is to maximize the amount of absorbed energy E_{abs} using the following cost function

$$\max(E_{abs}) = -\min \int_{t_1}^{t_2} (\sqrt{R_u^2 + S_u^2})\, \dot{z}^2(t)\, \mathrm{d}t \tag{16}$$

where $[t_1\ t_2]$ is the time span at which the cost function is evaluated.

Figure 2. The Gaussian MFs updating principle.

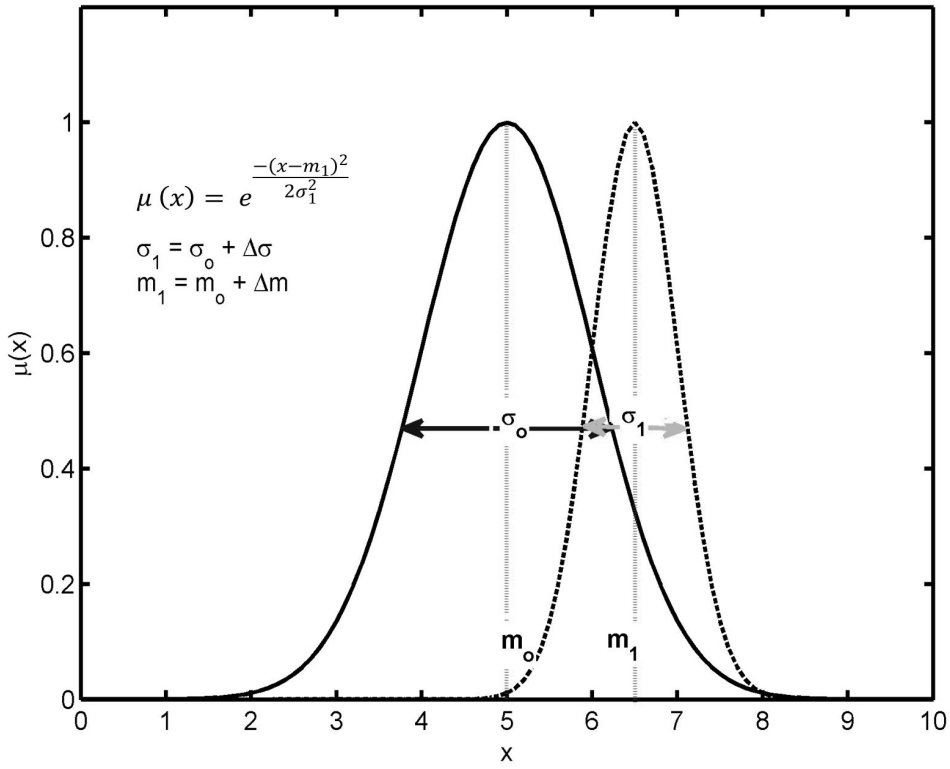

Figure 3. Block diagram of the proposed PSO-FLC controller.

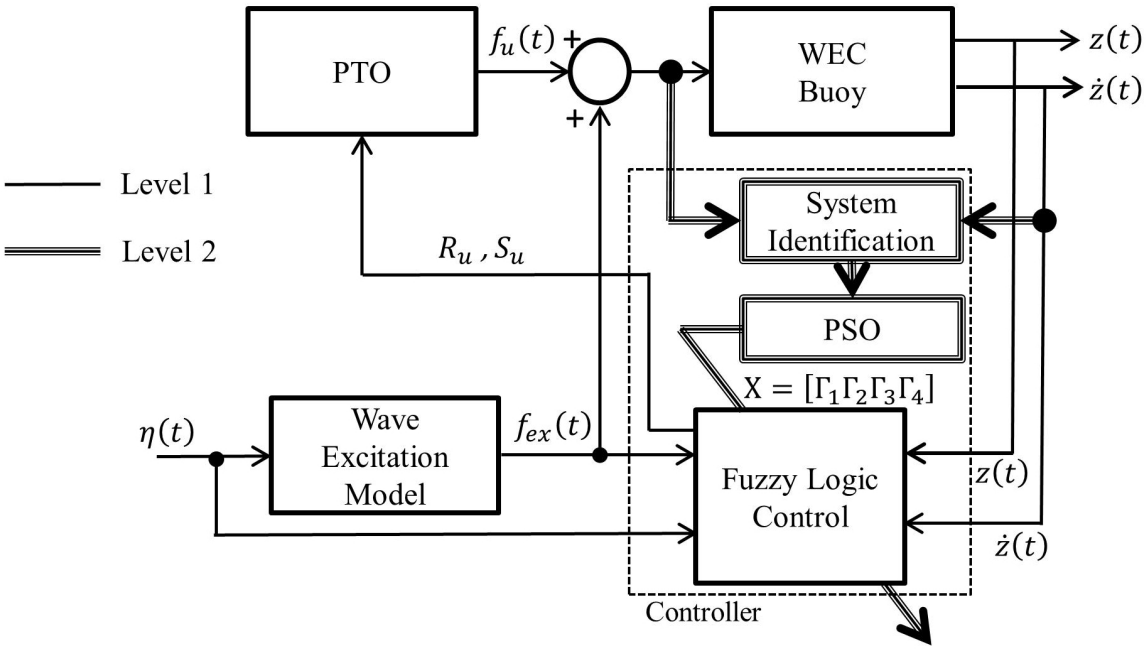

The control regime consists of two levels with separate time scales as shown in Figure 3. In the first level, the control law is issued at every sampling instant using the most recent FIS update. While in the second level, the FIS is updated at a lower rate in which the cost function shown in Equation (16) is maximized . To reduce the computational complexity and ease the controller real-time applicability, the optimization is carried out for a trajectory of the most recent wave samples (*i.e.*, in last 10 s), which is adequate, knowing the frequency at which most energetic sea waves propagate. To accommodate the effects of the nonlinear dynamics, system uncertainties and the stochastic behavior, it is crucial to update the system model, in order to allow the PSO algorithm to correctly modify the fuzzy controller based on the most recent model. System identification is performed prior to running the PSO. Here, the wave-buoy interaction is modeled as a single input single output black-box auto-regression model, such as [36]

$$y(t) + a_1 y(t-1) + \ldots + a_{n_a} y(t-n_a) = b_1 u(t-1) + \ldots + b_{n_b} u(t-n_b) + e(t) \tag{17}$$

where $y(t)$ is the buoy vertical velocity and $u(t)$ represents the summation of $f_{ex}(t)$ and $f_u(t)$, while $e(t)$ models the measurement noise. The parameters n_a and n_b are the number of poles and zeros, respectively. Therefore, the estimated output can be written as [36]

$$\hat{y}(t|\theta) = \theta^T \phi(t) \tag{18}$$

where

$$\theta = [a_1\ a_2\ \ldots\ a_{n_a}\ b_1\ \ldots\ b_{n_b}]^T$$
$$\phi = [-y(t-1)\ \ldots\ -y(t-n_a)\ u(t-1)\ \ldots\ u(t-n_b)]^T$$

Note that no prediction algorithm is used in this work, hence the excitation force is considered to be ideally predicted. Also, it is worthy to mention that the PTO is assumed to have ideal conversion efficiency, that is no electrical losses are considered. Here, the controller should guarantee a stable operation of the system in all sea conditions, while implicitly respecting the physical limitations of the WEC.

4. Results and Discussion

To assess the proposed controller, numerical simulations are carried out using MATLAB/Simulink environment. Passive reactive control (PRC) regime is used as a simple and low cost strategy to further assess the developed fuzzy controllers. The PRC regime has been designed to maximize the captured power at only a single wave frequency. For this study, the PRC force is formulated similar to Equation (11), where R_u and S_u are tuned for a monochromatic sea state of T_p = 8 s and H_s = 2 m, which are 50 kN.s/m and 600 kN/m, respectively. To unify the operating conditions for all tested controllers, mechanical end-stop is deployed to limit the buoy maximum excursion to 3 m. Numerous sea state scenarios are generated and the performance of the heaving WEC is evaluated. Polychromatic sea states, that is, they contain more than one frequency component, have been utilized to assess the effectiveness of the proposed controller. JONSWAP spectrum is used to generate realistic irregular growing sea states [37].

4.1. Simulation Setup

The performance of the suggested PSO-FLC is compared with that of a FS-FLC and the PRC strategy. The hydrodynamic frequency domain analysis is carried out once before running the time domain simulations. The system design parameters are shown in Table 3. It is not easy to determine accurately the value of C_D, however, in this work it is set to 0.5, in an attempt to approximately make the drag force equal to half of that of the radiation force for a buoy velocity of 2 m/s.

Table 3. WEC design parameters.

Parameter (Symbol)	Value	Unit
Buoy radius (r)	5	m
Buoy mass (m_b)	2.68×10^5	kg
Water plane area (A_w)	78.54	m^2
Submerged volume (V_s)	261.80	m^3
Drag coefficient (C_D)	0.5	-
Buoyancy stiffness coefficient (S_b)	7.89×10^5	N/m
Restoring stiffness coefficient (S_{rs})	2×10^5	N/m
Added infinite mass (m_∞)	1.34×10^5	kg
Resonance angular frequency (ω_o)	1.56	rad/s
Seabed depth (d)	80	m
Losses resistance (R_l)	0.4×10^5	N.s/m
Mooring stiffness coefficient (S_m)	1.5×10^5	N/m
Mooring cable length (L_m)	4	m

The PSO population size is set to 50 particles, while the total number of searching iterations is set to 80. Maximum number of search iterations is determined such that a good balance is achieved between reaching an optimum or nearly optimum solution and reducing the computational burden. Other parameters like ω_n, β_1 and β_2 are set to 0.5, 0.4, and 1.2, respectively. A fixed step ode4 solver is chosen to compute the dynamic responses over 140 s time span and time step of 0.1 s. The FIS optimization requires around 20 s to be solved using a 3.16 GHz dual core processor. Hence the fuzzy MFs are updated every 20 s, that is approximately equivalent to two low-frequency waves.

4.2. Simulation Results

First, a polychromatic sea state of a significant wave height H_s of 1.25 m and a peak period T_p of 9 s is applied on the WEC. The performance of the proposed PSO-FLC along with those of the FS-FLC and the PRC are shown in Figure 4. The buoy's vertical displacement and velocity responses are fairly close for all controllers in the first 40 s; however, beyond t = 90 s, there are significant discrepancies. In Figure 5a, it can be noticed that the proposed PSO-FLC produces the best performance in terms of the amount of averaged absorbed power, which is approximately 72 kW, while FS-FLC and PRC produce 61 kW and 53 kW, respectively. Note that, although the PSO-FLC controller has close average-to-peak ratio (4.8%) to the FS-FLC controller (5.2%), it has produced 15% more average power than its counterpart. That clearly shows the importance of managing the available control resource, which both controllers share in common.

Figure 4. The dynamics of the WEC buoy under different controllers (**a**) wave elevation; (**b**) buoy displacement; (**c**) buoy velocity.

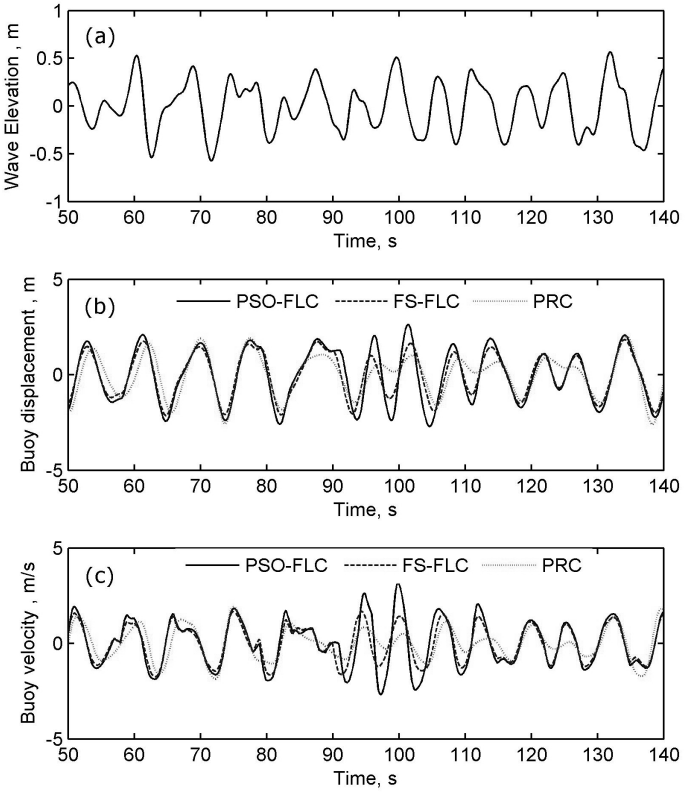

Figure 5. The instantaneous absorbed power (black) along with the corresponding time-averaged power (grey) (**a**) PSO-FLC; (**b**) FS-FLC; (**c**) PRC.

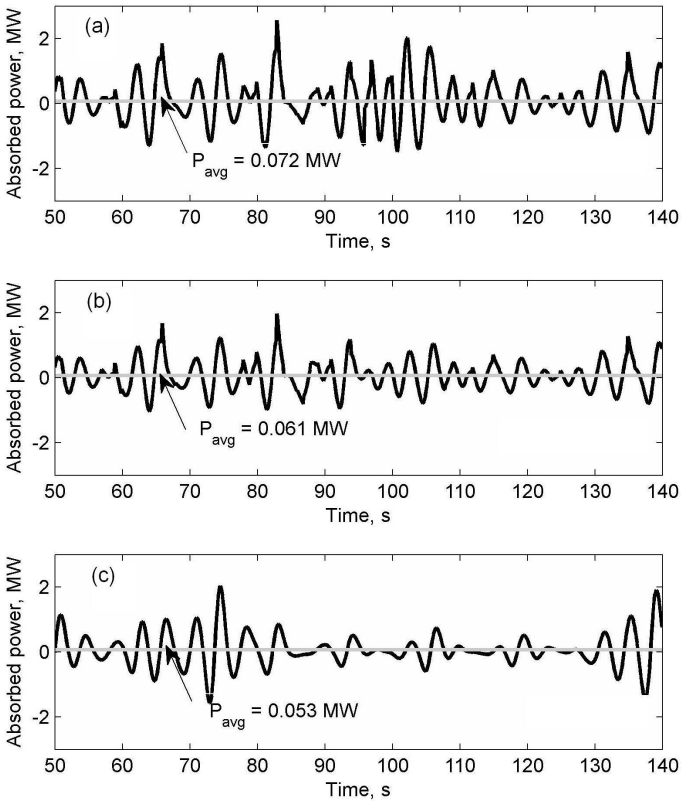

Figure 6 shows the dynamics of the PTO system, namely, the damping, stiffness, and the overall control force for the three controllers. As shown in Figure 6a, the PSO-FLC produced a time averaged damping of 54 kN.s/m, while the FS-FLC produced more damping that is 58 kN.s/m. As for the stiffness force, it is the opposite, the PSO-FLC produced 6% more than the FS-FLC. Despite that both of the PSO-FLC and the FS-FLC have similar damping and stiffness capacity, the self-configurable nature of the PSO-FLC enables it to utilize the available control resource efficiently, resulting in capturing more energy.

Figure 6. The dynamics of the WEC PTO (**a**) damping coefficient; (**b**) stiffness coefficient; (**c**) PTO control force.

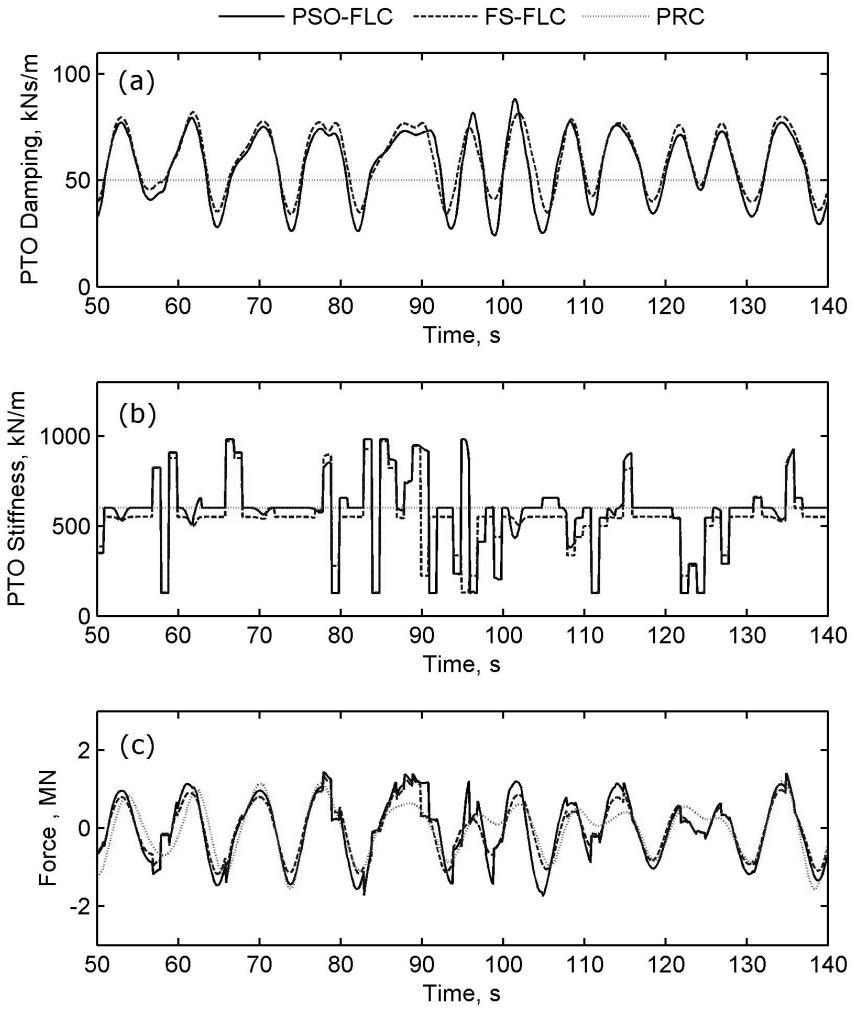

The control strategies performance subject to varying wave frequency is presented in Figures 7 and 8. In Figure 7, the applied waves have height of 1 m. Note that the PSO-FLC has better overall performance in terms of the averaged absorbed power than both of FS-FLC and the PRC. The PSO-FLC maintains nearly fixed advantage in the average absorbed power of approximately 11%, especially, at $0.6 \leq \omega \leq 0.95$. The reason for poor power absorption at very low wave frequency is the limited reactive capacity of the PTO. That is, as the wave period increases the PTO is required to issue more reactive power, in order to force the buoy to become in phase with the excitation force. The PRC produces superior performance around the frequency at which it is tuned, while the fuzzy-based controllers

produced wider absorption bandwidth. As shown in Figure 7b, the PSO-FLC failed to compete with FS-FLC in terms of the average-to-peak ratio, especially beyond ω = 0.6 rad/s. Note that at low wave frequency, the average-to-peak ratio is small indicating the generation of large reactive power, which agrees with our previous observation. The average normalized PTO coefficients are shown in Figure 7c,d, which shows almost steady trajectory for the damping coefficient, which is intuitive knowing that the wave height is fixed. However, the stiffness coefficient suffers from monotonic decrease as ω increases, indicating the need for lower reactive force. Also, notice that the stiffness coefficient becomes lower than the PRC fixed stiffness coefficient at $\omega \geq 0.8$ rad/s . The reason is that less stiffness is required at large wave frequencies, which is even lower than its PRC counterpart, knowing that the PRC is tuned at H_s= 2 m and ω = 0.8 rad/s.

Figure 7. Comparison of the controllers performance for sea-states with H_s = 1 m and varying wave frequency (**a**) average absorbed power; (**b**) average-to-peak power ratio; (**c**) normalized PTO damping; (**d**) normalized PTO stiffness.

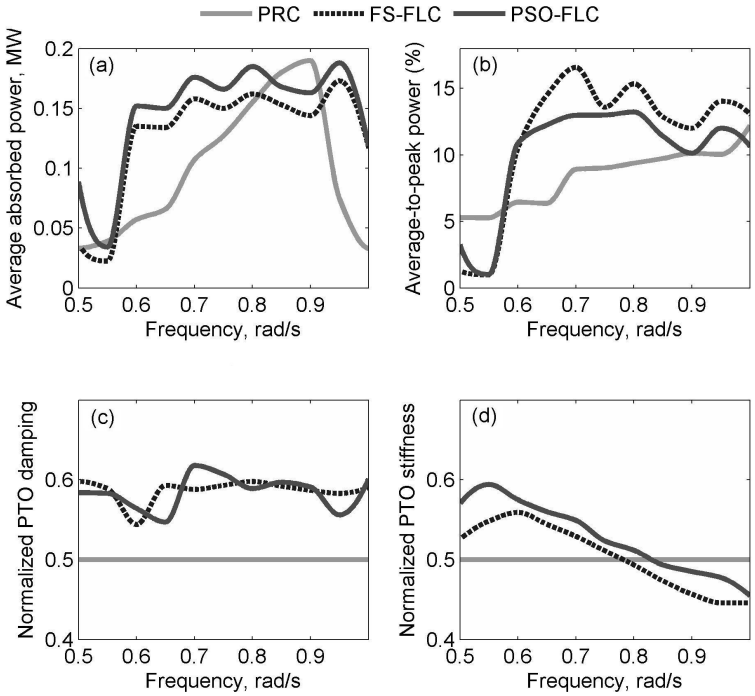

The previous analysis is repeated for waves with larger heights (H_s = 3 m) as depicted in Figure 8. Similarly, the PSO-FLC manages to produce more power for $\omega \geq 0.6$ rad/s. It can be observed that the average-to-peak ratio trajectories dropped significantly, compared to the case when H_s = 1 m. That is due to the significantly larger reactive power content. As expected, both the damping and stiffness coefficients are larger than the PTO coefficients produced by the PRC strategy across all wave frequencies.

Next, various irregular sea states were applied on the buoy. These sea states have been categorized based on the significant wave height H_s, the wave peak frequency ω_p, and the wave bandwidth. In terms of H_s, the sea states were divided to soft, moderate, and rough, corresponding to, 1.25 m, 2.25 m, 3.25 m, respectively. While two wave periods were considered, long and short, corresponding to a wave period of 7 s and 11 s, respectively. Also, the wave bandwidth has been divided into two sets, broad and narrow as shown in Figure 9.

Figure 8. Comparison of the controllers performance for sea-state with H_s = 3 m and varying wave frequency (**a**) average absorbed power; (**b**) average-to-peak power ratio; (**c**) normalized PTO damping; (**d**) normalized PTO stiffness.

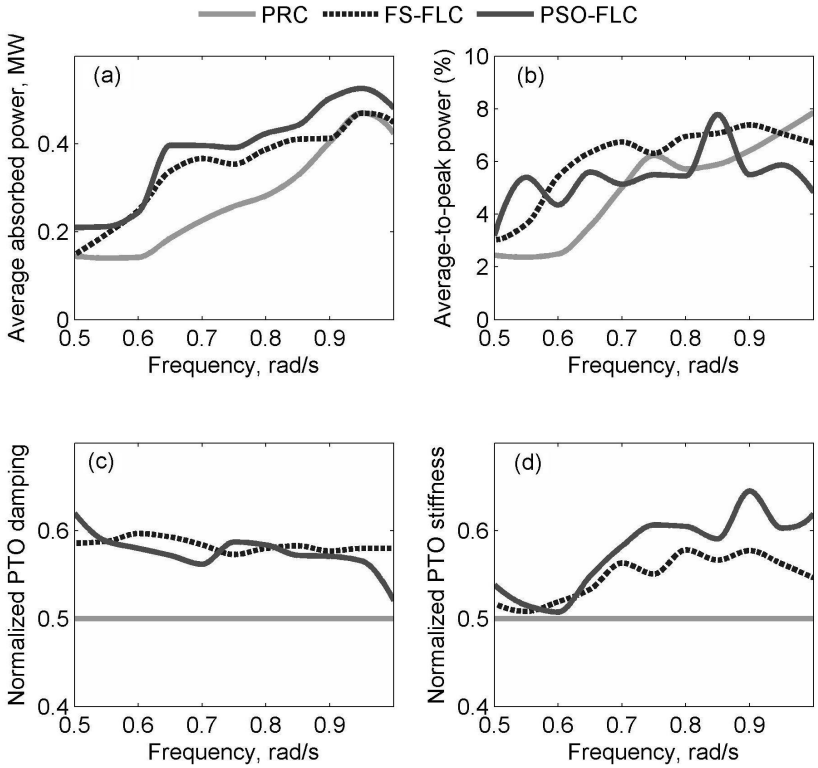

Figure 9. Jonswap wave spectrum of a sea-state with T_p= 11s and H_s = 2.25 m, broad bandwidth (solid) narrow bandwidth (dashed).

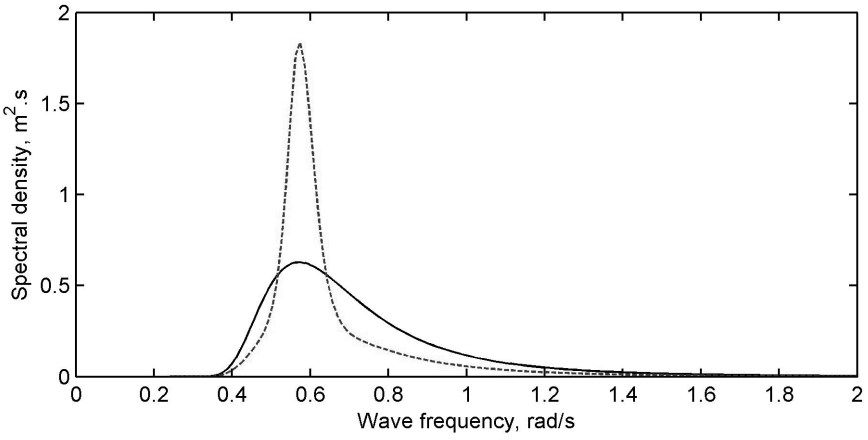

Figure 10 summarizes the performance of the controllers at all of the sea states based on the amount of averaged absorbed power. Clearly the PSO-FLC has produced more power at all sea states. Note that at Figure 10a, when the applied wave has a long period and narrow bandwidth, the PRC is more competitive, which is expected since the applied wave firmly falls into the controller bandwidth. However, when a broad wave is applied, the PRC becomes less productive as shown in Figure 10b. With T_p = 7 s as shown in Figure 10c,d, the fuzzy based controllers clearly outperformed the PRC, since they have a broader absorption bandwidth.

Figure 10. WEC power absorption at different sea-state scenarios (**a**) long period narrow bandwidth; (**b**) long period broad bandwidth; (**c**) short period narrow bandwidth; (**d**) short period broad bandwidth.

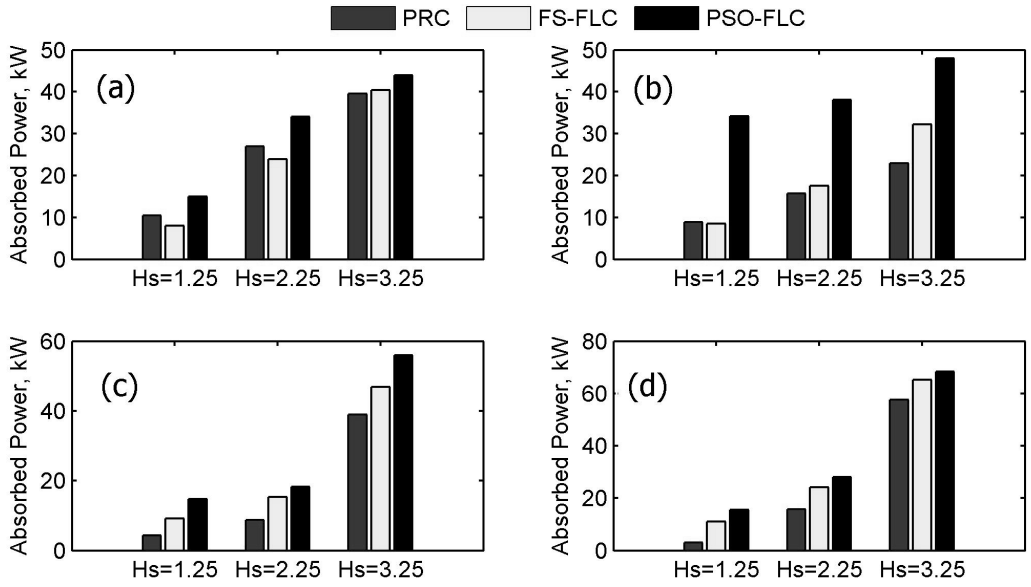

Figure 11. Controller sensitivity to variations in the mooring stiffness coefficient under a sea-state of H_s = 1.25 m (**a**) T_p = 11 s; (**b**) T_p = 7 s.

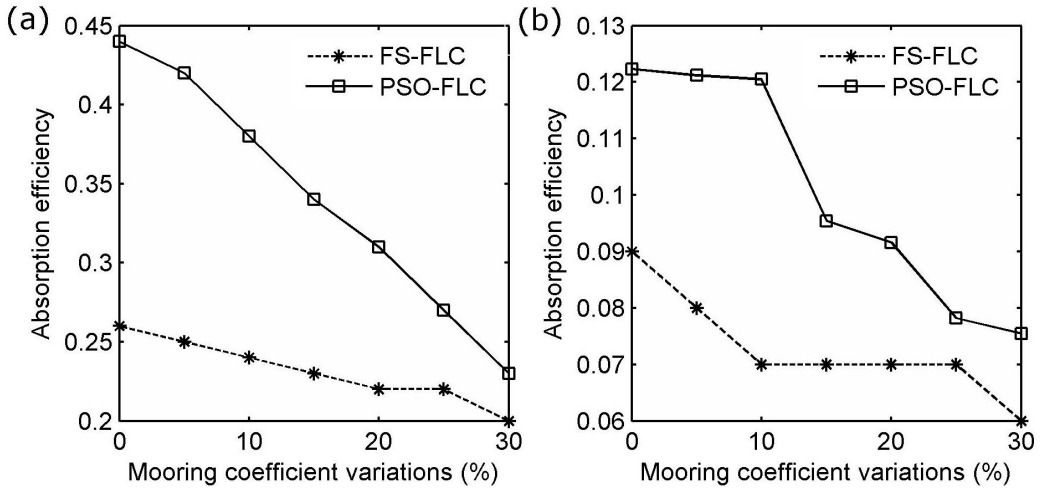

The sensitivity of the proposed controller towards parameter variations is assessed. Generally, controllers which are independent of the system mathematical model exhibit certain level of robustness, such as fuzzy logic controllers. However, a rigorous analytical approach is difficult to attain. Intuitively, the adaptive nature of the PSO-FLC is expected to further make the controller less sensitive to uncertainties. To showcase the controller sensitivity to variations in the plant parameters, the mooring stiffness coefficient S_m is varied for two different irregular wave environments. The reason of applying variations on S_m originates from the difficulty of accurately modeling its dynamics, hence it encompasses good deal of uncertainty. The absorption efficiency, which is the ratio of the average absorbed power to the average incident wave power, is used as a performance metric as shown in Figure 11. Since the controller is not designed to track a specific reference signal, the controller robustness is evaluated based on the degree of deterioration in the absorption efficiency. It can be observed that the proposed

PSO-FLC has the upper hand over the FS-FLC for all variations in S_m for both sea-states. Nevertheless, the PSO-FLC is more sensitive to variations in S_m when waves of longer periods are applied. That is expected, since long period waves are more energetic, which makes the controller find it difficult to issue more force from the PTO, hence the efficiency drops and part of the incident energy is returned back to the sea. In Figure 11a, the PSO-FLC suffers from rapid monotonic deterioration in the absorbed efficiency as the ΔS_m is increased, where 30% increase in S_m has resulted in 47% drop in efficiency, while only 23% drop is recorded for FS-FLC. On contrary, at T_p = 7 s, the maximum efficiency drop is 38% for PSO-FLC compared to 33% for the FS-FLC. Note in Figure 11b, the PSO-FLC suffers from slight degradation in the absorption efficiency up to 10% increase in S_m, this is due to the availability of extra control resource in the PTO, which is operating far from its physical limitations.

5. Conclusions

In this paper, an intelligent fuzzy logic controller for single body heaving WECs is proposed. The suggested controller has the ability to update its internal structure by continuously modifying the fuzzy MFs using PSO algorithm. Several polychromatic sea states are applied to the system and the PSO-FLC proved its superiority to FS-FLC. The PSO-FLC is capable of forcing the WEC system to absorb more energy regardless of the characteristics of the incoming waves. Also, the proposed controller can keep the system oscillations within reasonable bounded excursions, hence keeping the system stable.

It is obvious from the results that the PSO-FLC strategy utilizes more control resource (*i.e.*, PTO force) than the FS-FLC, even thought, both control strategies were designed with the same damping and stiffness limitations. Moreover, it has been shown that the proposed PSO-FLC strategy produced high average-to-peak ratio comparable to that of FS-FLC, while outperforming other control strategies in the amount of average absorbed power. This indicates that the PSO-FLC has better capability in using the available PTO force compared to both FS-FLC and PRC. Due to the irregularity and ambiguity of the sea environment, having such a tunable controller is essential to avoid the over-sizing of the PTO rating, therefore, enhancing the economic feasibility of the proposed solution.

The robustness of the PSO-FLC has been addressed through applying various perturbations to the system, which proved that robustness to parameter variations is function of the characteristics of the wave environment. It is important to mention that optimum operation of the WEC cannot be achieved; however, operating the system near the optimal condition as long as possible is conceivable. Also, due to the meta-heuristic nature of the PSO algorithm, reaching to an optimal solution is not guaranteed. In this study, the design parameters of the PSO algorithm are kept constant throughout the simulations. A possible improvement, which will be the subject of future research, would be using an adaptive PSO algorithm, where the parameters that determine the searching behavior and convergence speed of the PSO algorithm can be updated online. Combining short-term prediction algorithms to the current controller would probably alleviate the problem of real-time applicability, where enough time can be given to the PSO algorithm to optimize the fuzzy controller, these and other topics would be the scope of future work.

Author Contributions

This work is part of the doctoral research conducted by Mohammed Jama and supervised by Hassan Noura. Addy Wahyudie contributed in designing the fuzzy controller. Hassan Noura and Ali Assi have verified the theoretical soundness of the proposed control strategy. All co-authors had substantial contributions in writing and proofreading the manuscript.

Conflicts of Interest

The authors declare no conflict of interest.

References

1. Valerio, D.; Beirao, P.; Mendes, M.J.G.; Sa da Costa, J. Comparison of control strategies performance for a wave energy converter. In Proceedings of the 2008 16th Mediterranean Conference on Control and Automation, Ajaccio, France, 25–27 June 2008; pp. 773–778.
2. Falcao, A.F.O. Wave energy utilization: A review of the technologies. *J. Renew. Sustain. Energy Rev.* **2010**, *14*, 899–918.
3. Price, A. New Perspectives on Wave Energy Converter Control. Ph.D. Thesis, University of Edinburgh, Edinburgh, UK, 2009.
4. Babarit, A.; Clement, A.H. Optimal latching control of a wave energy device in regular and irregular waves. *Appl. Ocean Res.* **2006**, *28*, 77–91.
5. De La Villa JaÃl'n, A.; Andrade, D.E.M.; Santana, A.G. Increasing the efficiency of the passive loading strategy for wave energy conversion. *J. Renew. Sustain. Energy* **2013**, *5*, doi:10.1063/1.4824416.
6. Tedeschi, E.; Molinas, M. Tunable control strategy for wave energy converters with limited power takeoff rating. *IEEE Trans. Ind. Electron.* **2012**, *59*, 3838–3846.
7. Slotine, J.; Li, W. *Applied Nonlinear Control*; Prentice Hall: Englewood Cliffs, NJ, USA, 1991.
8. Valerio, D.; Mendes, M.J.G.C.; Beirao, P.; da Costa, J.S. Identification and control of the AWS using neural network models. *J. Appl. Ocean Res.* **2008**, *30*, 178–188.
9. Brekken, T. On model predictive control for a point absorber wave energy converter. In Proceedings of the 2011 IEEE Trondheim PowerTech, Trondheim, Norway, 19–23 June 2011; pp. 1–8.
10. Schoen, M.P.; Hals, J.; Moan, T. Wave prediction and robust control of heaving wave energy devices for irregular waves. *IEEE Trans. Sustain. Energy* **2011**, *26*, 627–638.
11. Jama, M.; Wahyudie, A.; Noura, H.; Assi, A. Fuzzy logic based reactive controller for heaving wave energy converters. In Proceedings of the 2012 International Conference on Renewable Energies for Developing Countries (REDEC), Beirut, Lebanon, 28–29 November 2012; pp. 1–5.
12. Jama, M.; Wahyudie, A.; Noura, H.; Assi, A. Self-tunable fuzzy logic controller for the optimization of heaving wave energy converters. In Proceedings of the 2012 International Conference on Renewable Energy Research and Applications (ICRERA), Nagasaki, Japan, 11–14 November 2012; pp. 1–6.

13. Kukolja, D.; Kuzmanovica, B.; Levi, E. Design of a PID-like compound fuzzy logic controller. *Eng. Appl. Artif. Intell.* **2001**, *14*, 785–803.
14. Stalberg, M.; Waters, R.; Danielsson, O.; Leijon, M. Influence of generator damping on peak power and variance of power for a direct drive wave energy converter. *J. Offshore Mech. Arct. Eng.* **2008**, *130*, doi:10.1115/1.2905032.
15. Falnes, J. Principles for capture of energy of ocean from ocean waves. Phase control and optimum oscillation. *Norw. Mar. Res.* **1976**, *6*, pp. 1–8.
16. Falnes, J. *Ocean Waves and Oscillating Systems*; Cambridge University Press: Cambridge, UK, 2002.
17. Markus, R.; Mario, E.; Oliver, S.; Brekken, T. Nonlinear model predictive control of a point absorber wave energy converter. *IEEE Trans. Sustain. Energy* **2013**, *4*, 118–126.
18. Jordan, M.A.; Beltran-Aguedo, R. Optimal identification of potential radiation hydrodynamics for moored floating structures-A new general approach in state space. *Ocean Eng.* **2004**, *31*, 1859–1914.
19. Cummins, W.E. The impulse response functions and ship motions. *Schiffstechnik* **1961**, *9*, pp. 101–109.
20. Ogilvie, T. Recent progress towards the understanding and prediction of ship motions. In Proceedings of the 5th Symposium on Naval Hydrodynamics, Bergen, Norway, 10–12 September 1964; pp. 3–80.
21. WAMIT User Manual. Available online: http://www.wamit.com/manual.htm (accessed on 12 March 2013).
22. Taghipoura, R.; Pereza, T.; Moan, T. Hybrid frequency-time domain models for dynamic response analysis of marine structures. *Ocean Eng.* **2008**, *35*, 685–705.
23. Backer, G.D. Hydrodynamic Design Optimization of Wave Energy Converters Consisting of Heaving Point Absorbers. Ph.D. Thesis, Ghent University, Zwijnaarde, Belgium, 2009.
24. Azadegan, A.; Porobic, L.; Ghazinoory, S.; Samouei, P.; Kheirkhah, A.S. Fuzzy logic in manufacturing: A review of literature and a specialized application. *Int. J. Prod. Econ.* **2011**, *132*, 258–270.
25. Coban, R.; Can, B. A trajectory tracking genetic fuzzy logic controller for nuclear research reactors. *Energy Convers. Manag.* **2010**, *51*, 587–593.
26. Karuppanan, P.; Mahapatra, K.K. PI and fuzzy logic controllers for shunt active power filter-A report. *ISA Trans.* **2012**, *51*, 163–169.
27. Emani, M.R.; Golenberg, A.A.; Turksen, I.B. Fuzzy logic control of dynamic systems: From modeling to design. *Eng. Appl. Artif. Intell.* **2000**, *13*, 47–69.
28. Shayeghi, H.; Jalili, A.; Shayanfar, H.A. Multi-stage fuzzy load frequency control using PSO. *Energy Convers. Manag.* **2008**, *49*, 2570–2580.
29. Chang, Y.; Wu, Y. The genetic algorithm based tuning method for symmetric membership functions of fuzzy logic control systems. In Proceedings of the International IEEE/IAS Conference on Industrial Automation and Control: Emerging Technologies, 1995, Torino, Italy, 22–27 May 1995; pp. 421–428.

30. Chiou, J.-S.; Tsai, S.-H.; Liu, M.-T. A PSO-based adaptive fuzzy PID-controllers. *Simul. Model. Pract. Theory* **2012**, *26*, 49–59.
31. Rama Mohan Rao, A.; Sivasubramanian, K. Multi-objective design of fuzzy logic controller using a self-configurable swarm intelligence algorithm. *Comput. Struct.* **2008**, *86*, 2141–2154.
32. Jamaludin, J.; Rahim, N.A.; Hew, W.P. Development of a self-tuning fuzzy logic controller for intelligent control of elevator systems. *Eng. Appl. Artif. Intell.* **2009**, *22*, 1167–1178.
33. Yang, X.S. *Engineering Optimization: An Introduction With Metaheuristic Applications*; John Wiley & Sons: Hoboken, NJ, USA, 2010.
34. Lee, K.Y.; El-Sharkawi, M.A.; Eds. *Modern Heuristic Optimization Techniques: Theory and Applications to Power Systems*; Wiley-IEEE Press: Piscataway, NJ, USA, 2008.
35. Kennedy, J.; Eberhart, R.C.; Shi, Y. *Swarm Intelligence*; Morgan Kaufman Publishers: Burlington, MA, USA, 2001.
36. Ljung, L. *System Identification, Theory for the User*; Prentice Hall: Englewood Cliffs, NJ, USA, 1999.
37. Kumar, V.; Kumar, K. Spectral characteristics of high shallow water waves. *Ocean Eng.* **2008**, *35*, 900–911.

© 2014 by the authors; licensee MDPI, Basel, Switzerland. This article is an open access article distributed under the terms and conditions of the Creative Commons Attribution license (http://creativecommons.org/licenses/by/3.0/).